CHAPTER IV
SYNTHESIS OF ACTIVATED CARBON

4.1 Raw materials

In this experiment, eucalyptus bark was used for the preparation of activated carbon by the phosphoric acid activation method. The eucalyptus bark was crushed and sieved through the mesh number 10 (approx. 2.0 mm) before being treated. The pictures of eucalyptus bark and activated carbon from eucalyptus bark are shown in Figure 4.1(a-b) which indicated that eucalyptus bark could be converted to activated carbon. Table 4.1 shows the ultimate analysis of the eucalyptus bark from the CHNS/O analyzer which revealed that eucalyptus bark had relatively high carbon content (more than 40%). Results from the proximate analysis obtained by chemical methods indicated low ash content at less than 1.35%. This was in the same range as those reported in literatures (Vesterinen 2003; Mészáros et al. 2004). This suggested that this precursor was suitable for the preparation of activated carbon.

4.2 Experiments

Experiments in this chapter included the preparation of activation carbon (Section 3.2.2) and the properties analysis of activated carbon (Section 3.2.3).

4.3 Optimal activation temperature

The effect of activation temperature was carried out at various temperatures: 350, 400, 450, 500, 550 and 600°C for 1 h using the weight by volume ratio of raw material and phosphoric acid (impregnation ratio) of 1:1. The results of these experiments are shown in Table 4.2.

4.3.1 Yield and bulk density

Table 4.2 demonstrates that % yield and bulk density of the activated carbon slightly decreased with increasing activation temperature. This could potentially be due to the removal of some components, e.g. tar like matter and phosphoric acid deposited in pore which occurred better at higher activation temperature, leading to the development of porosity. That is to say that an increase in activation temperature accelerated the development of porosity within the carbon structure.

4.3.2 Ash content

The ash contents of activated products obtained in this study are in the range of 5–6%. The changes in %ash content with activation temperature were due to the changes in the weight of compounds resided in the matrix of carbon. As ash content increased with temperature (see Table 4.2), this could imply that the other volatile components were removed at the rate faster than the un-combustible constituents like silica. This finding agreed well with that of Melnikov et al (2003) who stated that an increase in the ash content was due to the formation of some insoluble silica species with the presence of derived phosphoric acid-based species at high temperatures.

4.3.3 Specific surface area

The results summarized in Table 4.2 demonstrate that BET surface area increased gradually with activation temperature up to 500°C. It was observed that at the activation temperature of 500°C, well developed, uniformly sized pores were generally distributed throughout the matrix (Figure 4.2 (d)). The pore size distribution of activated is governed by the method of activation and is understood to be one of the critical factors which determines its sorptive capacity (Blache et al., 2000). Also, the shape of the pores is known to be affected by the kind and physicochemical characteristics of raw material (Jagtoyen and Derbyshier, 1998). Figure 4.3(a) shows that there were almost no pores for the activated carbon prepared at 350°C. As the activation progressed, pores were generated in greater extent and generally were enlarged. When the activation temperature was higher than 400°C (Figure 4.3(b) and (c)), the micropore structure of the activated carbon occurred in a greater extent. However, temperature above this point saw a declined in such area. This may be explained by the fact that thermal degradation occurred at temperatures >500°C, deteriorating its adsorption capacity and destroying the structure of the activated carbon, which resulted in the extinction of micropores (Figure 4.2 (e-f)). Generally, carbonization and activation temperature are recognized to have significant influence on the formation of pore structures of activated carbon, and this determines the adsorption capacity (Zhonghua and Vansant, 1995). Figure 4.3 (a-f) shows X-ray diffraction patterns of the activated carbon at various activation temperatures. At lower temperature, some hydrogen and carbon were removed due to the reaction with phosphoric acid and the stronger porous structure formed (Figure 4.3 (a) and (b)), whereas at higher temperature, the combination of biopolymers (cellulose, hemicelluloses and lignin) fragments took place. This destroyed the original cellulose,

hemicellulose and lignin structures and created the amorphous structure. At even higher temperatures (>500°C), the breakdown of structure bond of activated carbon seemed to occur, causing contraction and consequent reduction in porosity development. It was concluded, therefore, that an appropriate activation temperature for the production of activated carbon from eucalyptus bark was approximately 500°C. Effectively, BET surface area of activated carbon obtained in this condition was 1,354 $m^2 g^{-1}$.

4.3.4 Pore structure

Figure 4.4 illustrates N_2 adsorption isotherms on the activated carbon at different activation temperatures and an activation time of 1 h, respectively. At the lowest temperature (350°C), the shape of the adsorption isotherm was of Type II of the classification system originally mentioned by Brunauer et al. (1940) (abbreviated BDDT), with a well-defined plateau pointing to mesoporous structures. As activation temperature increased (>400 °C), the shapes of the curves gradually changed to feature the Type I isotherm, indicating the development of small pores. With an increase in activation temperature from 400 to 500°C, the nitrogen uptake increased quickly. Over 500°C, the rate of increase pore area became slow suggesting the widening of existing pores as well as the continuous creation of new pores. This was likely caused by the removal of volatile substances from the activation mixture due to pyrolysis and the rigorous reactions between activation agent and eucalyptus bark at higher activation temperature. The structural characterization results are summarized in Table 4.2. At temperatures below 350°C, the activated eucalyptus bark contained relatively low internal pores (59.42% micropore, 33.23% mesopore and 7.35% macropore). The pore development started to occur better as the temperature increased and reached the highest micropore fraction at 500°C (95.72%). Over 500°C, the development of pore became slow and losses in micropores were observed as shown in Table 4.2. The Horvath and Kawazoe's relative pressure of 0.95 indicated that the pore specific volume increased with an increase in activation temperature (but not beyond 500°C), the specific pore volumes were 0.043, 0.241, 0.762, and 1.091 $cm^3 g^{-1}$, at the activation temperatures of 350, 400, 450 and 500°C, respectively. At higher activation temperature than 500°C, the pore specific volume decreased with an increase in activation temperature due to a reduction in the amount of micropore. The pore specific volumes at activation temperature of 550 and 600°C were 0.950 and 0.931 $cm^3 g^{-1}$, respectively. Table 4.2 demonstrates that the pore size distribution and

pore volumes were highly dependent on the temperature. Under these conditions, activated carbon exhibited the highest micropore and total pore volume at the activation temperature of 500°C.

4.3.5 Iodine and methylene blue numbers

Iodine and methylene blue numbers are often employed to examine the adsorption capacity of the activated carbon. The iodine number gives an indication of the adsorption capacity of activated carbon in micropores (Jankowska et al., 1991) whereas the methylene blue number was used to represent mesoporous area. The iodine number of the standard of the commercial activated carbon is over 600 mg g^{-1} (TIS, 1989). Table 4.2 and Figure 4.5 demonstrate that an increase in activation temperature at a low temperature range (<500°C) significantly enhanced the iodine and methylene blue numbers of the activated carbon product. This could potentially be due to the removal of some components, e.g. tar-like matter, and phosphoric acid deposited in pore which occurred better at higher activation temperature, leading to the development of micropores and mesopores. At a higher temperature range (over 500°C), the quality of the activated carbon seemed to be deteriorated with temperature. This might be a result of the collapse of micropores which became more significant than the rate of increase in such pores at such high temperature, and resulting in the reduction of the iodine number. On the other hand, methylene blue number still increased significantly as the micropore was changed into mesopore which could still adsorb methylene blue.

In conclusion, the optimal temperature for the activation by phosphoric acid was 500 °C, the condition which gave the highest iodine and methylene numbers, and also BET surface area. Note that this condition also provided the highest percent of micropore.

4.4 Optimal weight by volume ratio of Eucalyptus bark and phosphoric acid (impregnation ratio)

The effect of impregnation ratio was investigated by varying the weight by volume ratio of eucalyptus bark and phosphoric acid from 1:0.3, 1:0.5, 1:0.8, 1:1, 1:2 and 1:3. The mixture was produced at the activation temperature of 500°C for 1 h. The results of these experiments are shown in Table 4.3 and are described below.

4.4.1 Yield and bulk density

Table 4.3 demonstrates that an increase in the amount of phosphoric acid during the activation process (lower impregnation ratio) resulted in a decrease in the % yield and bulk density of the activated carbon product. Phosphoric acid reacted with char and volatile matter and diffused quickly out of the surface of particles during the activation process. Therefore, with high phosphoric acid content, the gasification of surface carbon atoms became the predominant reaction which led to low carbon yield. A slightly lower bulk density of activated carbon product was also observed at high phosphoric acid content, and this was due to the difference in the pore structure of the carbon product as discussed later on.

4.4.2 Ash content

In general, ash content in activated carbon is not desirable and is considered an impurity. The ash content was estimated from the mass of the residue remained after combustion of the samples in air. Table 4.3 shows that %ash content of activated carbon decreased with decreasing impregnation ratio. It could be that phosphoric acid reacted with the contaminants in the eucalyptus bark, resulting in the removal of such impurity during the activation process. (as indicated in Section 4.3.2) As this removal process depended on the quantity of acid presented in the sample, significantly lower ash content was found in the conditions of high phosphoric acid content.

4.4.3 Specific surface area

The most important property of the activate carbon is its adsorptive capacity, which is related to the specific surface area. Generally, a higher surface area of the activated carbon allows a greater adsorptive capacity. The results summarized in Table 4.3 demonstrate that a higher level of BET surface area could be obtained from the activation with a higher amount of phosphoric acid. However, the BET surface area seemed to reach the highest value at the impregnation ratio of 1:1 and this formed an advanced pore network system as displayed in Figure 4.6(d). With an increase in the impregnation ratio, the material presented a less irregular surface as shown in Figure 4.7(a-c) which could be due to a lower quantity of activation agent available to react with eucalyptus bark and low amount of pore network as shown in Figure 4.6 (a-c). However, a higher amount of phosphoric acid caused some of the pores to enlarge or collapse, thus reducing BET surface area and porosity of activated carbon (Figure 4.7(e–f)). From XRD results in Figure 4.7, an increase in the mount of phosphoric acid led to a change in the chemistry of the carbon product, from a

patterned to amorphous structure. Higher impregnation ratios than 1:1 (e.g. 1:0.8 and 1:0.3) was found to lower the surface area and diminishing the adsorption characteristics particularly on methylene blue and iodine numbers. This was due to inadequate amount of phosphoric acid which was allowed to enter the reaction with eucalyptus bark during the activation process. In other words, results indicated that progressive development of porosity took place as more acid was incorporated into the precursor. However, this beneficial effect of increasing the impregnation ratio was likely to reach its limit as an excess of acid seemed to bring about collapse of pores and, therefore, structural contraction, presumably as a consequence of the intensified dilation. This excessive reaction was observed when the impregnation ratio became lower than 1:1.

Overall, it was suggested here that, for the activation of eucalyptus bark, the impregnation ratio should be 1:1.

4.4.4 Pore structure

Information on the carbon pore structure was derived from nitrogen adsorption isotherms obtained at -196°C using the surface area analyzer (Thermo Finnigan, Sorptomatic 1990). The shape of the adsorption isotherm can provide qualitative information on the adsorption process and the extent of the surface area available to the adsorbate. Nitrogen adsorption isotherms at -196°C (Figure 4.8 (a-f)) were found to follow Type I. Similarly, shaped isotherms were also obtained from other impregnation ratios, i.e. 1:0.3, 1:0.5, 1:0.8, 1:1, 1.2 and 1.3. All the isotherms followed Type I, indicating the existence of microporous structure where pore filling occurred at low relative pressures. An absence of hysteresis indicated the absence of mesoporosity. The shape of the isotherm knee could be used to estimate the size of the micropore (with the size of less than 2 nm) in the adsorbent using the Horvath-Kawazoe method (Horvath and Kawazoe, 1983) where the impregnation ratios of 1:0.3 and 1:1 resulted in activated carbon with the average micropore sizes of approx. 7.78 and 8.49 Å, respectively. These were considered to be within the microporous range, suggesting that the carbon products contained mostly micropores with only a small contribution of mesopore. Raising the amount of phosphoric acid led to a loss in micropores. This could be due to the collapse of micropore walls resulting in pore widening and an increase in mesopores portion. This was clearly illustrated in Table 4.3 where the fraction of micropore decreased with an increase in mesopore fraction as a result of an increase in the acid content during the activation process. Table 4.3

also illustrates that the pore specific volume increased with a decrease in the impregnation ratio, and at a relative pressure of 0.95, the specific pore volumes calculated from the Horvath and Kawazoe method with the data in Figure 4.8 were 0.420, 0.899, 1.080 and 1.091 cm^3g^{-1}, which seemed to be a logical sequence for the products at the impregnation ratios of 1:0.3, 1:0.5, 1:0.8 and 1:1.

4.4.5 Iodine and methylene blue numbers

Table 4.3 demonstrates that these parameters increased with a decrease in impregnation ratio, but not beyond the impregnation ratio of 1:1. As the acid content increased, more reaction took place, and consequently, more surface area was developed. From the discussion above, a higher acid led to a formation of the product with a higher level of volume and surface area which could then provide a higher adsorption capacity. Hence, iodine and methylene blue numbers increased with BET area. Differences between values of BET area and iodine number may be attributed to the larger molecular size of iodine than nitrogen. Table 4.3 illustrates that as the impregnation ratio decreased, the adsorption of methylene blue increased significantly. This indicated that there existed more mesopore at a higher level of acid than that at a lower acid content. The results on the adsorption of iodine and methylene blue supported the conclusion where the contribution of mesopore was more significant at a high acid content. This finding agreed well with those of Molina-Sabio et al. (1995) and Jagtoyen and Derbyshire (1998) who stated that chemical activation with phosphoric acid of different materials usually led to mesoporous carbons at low impregnation ratios.

The experimental results showed that the most appropriate weight by volume ratio of raw material and phosphoric acid (impregnation ratio) of eucalyptus bark for activation was 1:1. This activated carbon gave the highest iodine number, methylene blue number and BET surface area.

4.5 Optimal activation time

100 g of eucalyptus bark was impregnated into a 100 ml of phosphoric acid (85 wt%) (weight by volume ratio of raw material and phosphoric acid = 1:1), then carbonized in a muffle furnace at 500°C for 0.5, 1.5, 2, 2.5, and 3.0 h. The results of these experiments are shown in Table 4.4 and discussed below.

4.5.1 Yield and bulk density

Table 4.4 demonstrates that % yield of activated carbon decreased while activation time increased because of the loss of volatile matter. The gaseous product, volatile matter and phosphoric acid initially diffused out of the particle relatively rapidly (in the first 2 to 3 h). As the remaining volatile matter stayed deeper in the particle, it took a longer time to diffuse out. This finding revealed that the porosity developed quickly in the first 2 h then became more slowly through the course of activation process.

4.5.2 Ash content

Table 4.4 demonstrates that % ash content in activated carbon increased with activation time period. This could be that ash content remained quite inactive in the matrix whilst the eucalyptus bark reacted with phosphoric acid with more contact time leading to a more progressive gasification of the carbon content. The acidic properties of synthetic phosphoric acid activated carbons may be related to phosphorus containing compounds formed during activation. Possible candidates for such compounds may be polyphosphates. An excess of phosphoric acid remaining in pores after activation could also contribute to higher ash content.

4.5.3 Specific surface area

The results summarized in Table 4.4 demonstrate that a higher BET surface area (1,230 to 1,457 $m^2 g^{-1}$) was obtained when the activation time increased from 0.5 to 1.5 h. This was because the volatile matter and phosphoric acid diffused out rapidly especially at the external surface during the initial activation period. As a result, micropores and mesopores developed quickly. The effect of activation time on the development of surface area of the activated carbon product is represented in Figure 4.9 (a-f). The previous report by Mameri et al. (2000) could be used to describe the results here. In their work, it was mentioned that the percent micropore of the activated carbon was recognized to rise with activation time. After 1.5 h, the BET surface area slightly decreased because mesopores started to form inside the structure. It was under this condition that the porous structure of activated carbon deteriorated due to thermal degradation. The XRD patterns of the activated carbon showed almost no diffraction lines indicating they were all amorphous (Figure 4.11 (a-f)). Two broad peaks at low diffraction angles were observed to correspond to the diffraction angles 2θ at 20–22° and 36–43°, which were assigned to the disordered graphitic 002 and

100 planes, respectively (Kaneko et al., 1994). These illustrated that the pores contained microcrystallites, with intercrystallite and intracrystallite voids.

4.5.4 Pore structure

Figure 4.9 shows that nitrogen adsorption isotherms at -196°C for all samples followed Type I isotherm, indicating the existence of microporous structure. These adsorption isotherms clearly demonstrated the dominating microporous structure of the activated carbon product with some smaller fraction of mesopores. The activation time also exerted significant effects on the development of pore structure of the resulting carbons due to the opening of blocked pores and development and widening of micropore. This was obvious from the results shown in Table 4.4 which demonstrates an increase in microporosity when the activation time increased from 0.5 to 1 h. As the activation time increased from 1.5 to 3 h, the reduction in porosity was observed, and this was reflected by a decrease in surface areas and total pore volumes of the activated carbon, and was expected to be due to the over reaction and the resulting breakdown of cross-links within the carbon structures.

4.5.5 Iodine and methylene blue numbers

During the first 1.5 h of reaction, the iodine and methylene blue numbers increased in the same trend. This was due to the progressive reaction of phosphoric acid with the bark which generated a large number of new pores. After 1.5 h, the iodine number slightly decreased while methylene blue number still increased, although only slightly. At this time, micropores were expected to collapse, slightly increasing mesopores. BET surface area (Table 4.4) confirmed the changes in the development of micropores and mesopores.

The experimental results demonstrated that the optimum activation time was 1.5 h where the resulting activated carbon gave the highest iodine number and BET surface area.

4.6 Concluding remarks

The comparison of the carbon product from this work with the others with the same raw materials (Eucalyptus) was provided in Table 4.5. This comparison was based on the maximum iodine and methylene blue numbers, along with the specific surface area. It was found that the phosphoric acid activation could provide the activated carbon with relatively higher levels of methylene blue number and BET

surface area when compared to other activation methods. This was because phosphoric acid activation was a direct activation process which affected the formation of micropore and mesopore, and this resulted in higher levels of methylene blue number and BET surface area. The comparison between properties of activated carbon from various types of precursors as provided in Table 4.6 suggests that eucalyptus bark was a good choice for the preparation of activated carbon. These comparisons illustrate that Eucalyptus bark could be carbonized at a relatively short time interval and with a reasonably low acid fraction, and emphasizes the potential in the future development of such process.

Table 4.1 Analysis of eucalyptus bark

Proximate analysis (% by weight, dry basis)	
Fixed carbon	12.10
Volatile matter	76.05
Moisture	10.50
Ash	1.35
Ultimate analysis (% by weight)	
C	41.36
H	4.67
N	*

* low detection limit

Table 4.2 Characteristics of activated carbon form eucalyptus bark at various activation temperatures

Parameters		Temperature (°C)					
		350	400	450	500	550	600
Bulk density (g cm^{-3})		0.269	0.261	0.257	0.251	0.249	0.236
Ash content (%)		3.86 ± 0.11	3.97± 0.10	4.06± 0.08	4.88± 0.09	5.23± 0.05	5.97± 0.07
Yield (%)		28.45± 0.7	27.67± 0.5	27.01± 0.3	26.21± 0.8	25.78± 0.01	24.58± 0.3
Iodine number (mg g^{-1})		434.4± 4	621.9± 7	867.1± 7	1,043.4± 8	971.4± 8	935.8± 6
Methylene blue number (mg g^{-1})		408.6± 4	411.8± 1	425.0± 2	425.4± 2	425.9± 3	426.8± 2
BET Surface area (m^2 g^{-1})		17	280	857	1,354	1,251	1,186
Specific pore volume (cm^3 g^{-1})		0.043	0.241	0.762	1.091	0.950	0.931
Average pore diameter (Å)		450	19	47	8	61	112
Pore size distribution	micro (%)	59.42	91.74	89.17	95.72	88.46	89.21
	meso (%)	33.23	7.73	9.89	4.28	10.77	9.97
	macro (%)	7.35	0.53	0.94	0.00	0.77	0.82

Table 4.3 Properties of activated carbon prepared at various impregnation ratios

Parameters		Impregnation ratio					
		1:0.3	1:0.5	1:0.8	1:1	1:2	1:3
Bulk density (g cm^{-3})		0.255	0.252	0.252	0.251	0.251	0.250
Ash content (%)		6.64± 0.08	6.48± 0.11	5.86± 0.12	4.88± 0.09	4.40± 0.08	4.00± 0.12
Yield (%)		29.6± 0.6	28.7± 0.7	27.9± 0.5	26.2± 0.8	25.8± 0.6	25.2± 0.7
Iodine number (mg g^{-1})		610± 14	821± 21	929± 13	1,043± 8	1,004± 4	595±8
Methylene blue number (mg g^{-1})		299.2±3	364.3± 5	424.6± 1	425.4± 2	324.4± 1	89.3± 4
BET Surface area (m^2 g^{-1})		545	991	1,170	1,354	1,340	671
Pore specific volume (cm^3 g^{-1})		0.420	0.899	1.080	1.091	1.066	0.612
Average pore diameter (Å)		7.78	6.85	9.16	8.49	52.10	138.11
Pore size distribution	micro (%)	98.28	96.82	96.00	95.72	84.54	88.56
	meso (%)	1.72	3.18	4.00	4.28	14.27	10.74
	macro (%)	0.00	0.00	0.00	0.00	1.19	0.70

Table 4.4 Properties of activated carbon prepared at various activation times

Parameters		Activation times (h)					
		0.5	1.0	1.5	2.0	2.5	3.0
Bulk density (g cm^{-3})		0.279	0.251	0.247	0.234	0.221	0.219
Ash content (%)		3.75± 0.02	4.88± 0.09	4.92± 0.5	5.21± 0.10	5.92± 0.07	6.32± 0.06
Yield (%)		29.85± 0.6	26.2± 0.8	25.86± 0.3	24.24± 0.6	23.53± 0.4	22.54± 0.6
Iodine number (mg g^{-1})		800± 10	1,043± 8	1,226±1	1,124± 1	1,045±7	1,093±2
Methylene blue number (mg g^{-1})		424.4±1	425.4± 2	425.5± 1	425.4± 2	425.3± 2	425.4± 1
BET Surface area (m^2 g^{-1})		1,230	1,354	1,457	1,456	1,448	1,441
Specific pore volumes (cm^3 g^{-1})		1.081	1.091	1.241	1.201	1.221	1.143
Average pore diameter (Å)		30.07	8.49	53.97	35.69	28.70	28.49
Pore size distribution	micro (%)	88.32	95.72	87.80	85.64	87.23	87.57
	meso (%)	10.76	4.28	11.13	13.19	11.85	11.47
	macro (%)	0.92	0.00	1.07	1.17	0.92	0.96

Table 4.5 Comparison of Eucalyptus-derived activated carbons obtained from this work and other reports

Description	This work	Bello et al. (2002)	Jindaphunphairoth (2000)	Tancredi et al. (1996)	Arriagada et al.(1994)
Raw material	*Eucalyptus camaldulensis Dehn* bark	*Eucalyptus globules* wood	*Eucalyptus camaldulensis Dehn* wood	*Eucalyptus grandis* sawdust	*Eucalyptus globulus* wood
Carbonization	-	870°C for 2 h with N_2 and a heating rate of 4 °C min^{-1}	450°C and 45 min	800°C for 2 h with N_2 and a heating rate of 10 °C min^{-1}	450°C for 2 h
Activation	500°C for 1 h	600°C for 30 min	900°C for 2.5 h	800°C for 1 h	900°C for 4.5 h
Activating agent	Phosphoric acid	Carbon dioxide	Steam	Steam	Steam
% Yield	26	-	33	23	23
Iodine number (mg g^{-1})	1,226	-	1,233	-	968
Methylene blue number (mg g^{-1})	425	-	242	-	311
BET surface area (m^2 g^{-1})	1,457	-	1,076	1,190	1,193

Table 4.6 Comparison of phosphoric acid-derived activated carbons obtained from this work and other reports

Description	This work	Girgis and Ishak (1999)	Castro et al. (2000)	Diao et al. (2002)	Girgis et al. (2002)	Vernersson et al. (2002)	Daifullah et al. (2004)
Raw material	Eucalyptus bark	Cotton stalk	Sugar cane bagasse	Grain sorghum	Peanut hull	*Arundo donax* cane	Rice husk
Carbonization	-	-	-	300 °C for 15 min with N_2	-	-	-
Activation	500°C for 1 h	500°C for 2 h	500 °C for 1 h and heating rate of 3 °C min^{-1}	500°C for 15 min	500°C for 3 h	500°C for 1 h and heating rate of 3°C min-1	500°C for 2.5 h and heating rate of 10°C min^{-1}
Impregnation ratio	1:1 with 85% acid by weight	1:1.6 with 65% acid by weight	1:1.5 with mixed 28-60% acid by weight	1:0.76 with 15% acid by weight	1:1 with 85% acid by weight	1:2 with mixed 32-60% acid by weight	1:0.7 with 85% acid by weight
% Yield	26	-	-	29	22	-	-
Iodine number (mg g^{-1})	1,043	-	746	-	-	-	-
Methylene blue number (mg g^{-1})	425	-	283	-	384	-	-
BET surface area (m^2 g^{-1})	1,354	1,032	1,132	1,522	1,177	1,333	376

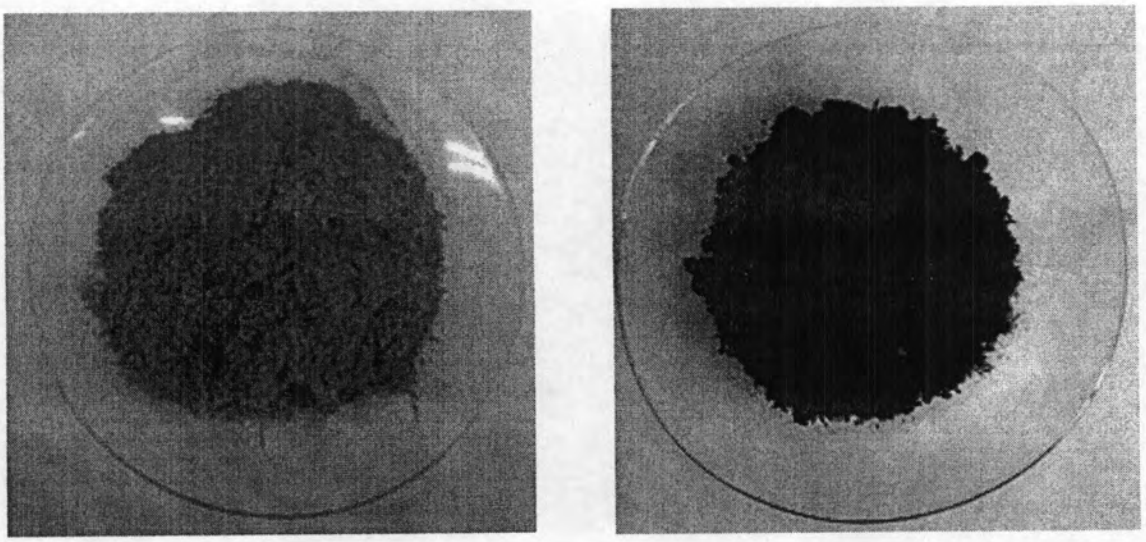

(a) (b)

Figure 4.1 (a) eucalyptus bark (b) activated carbon from eucalyptus bark

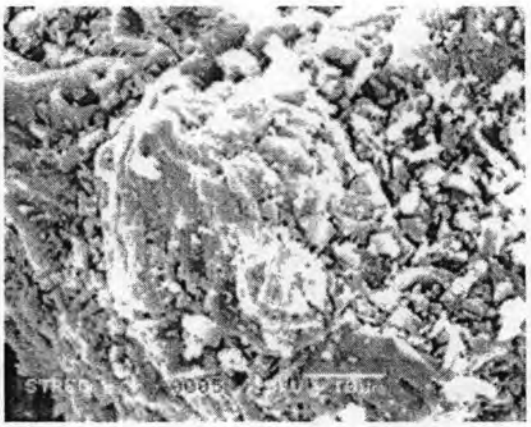

(a)

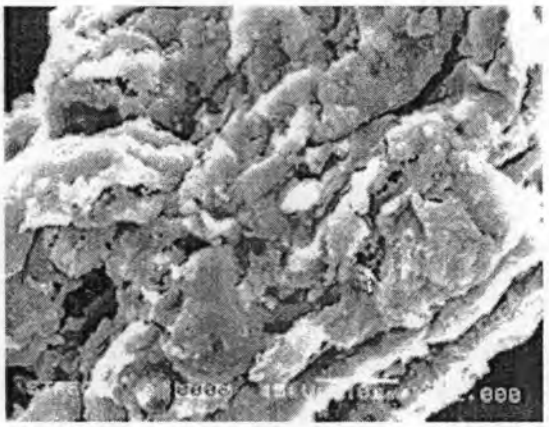

(b)

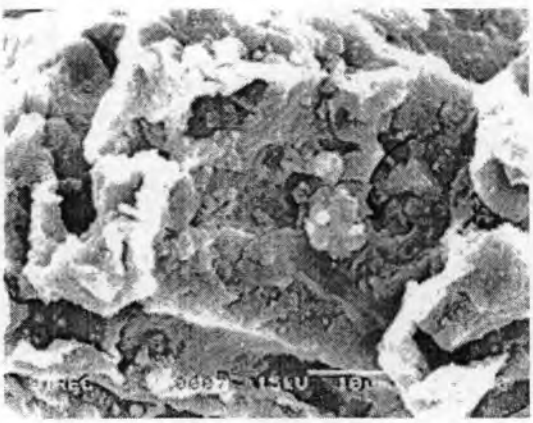

(c)

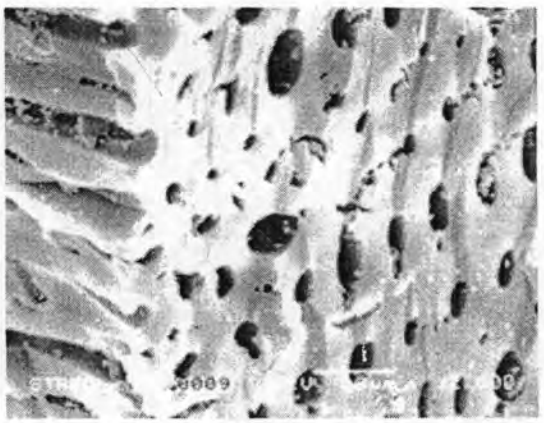

(d)

(e)

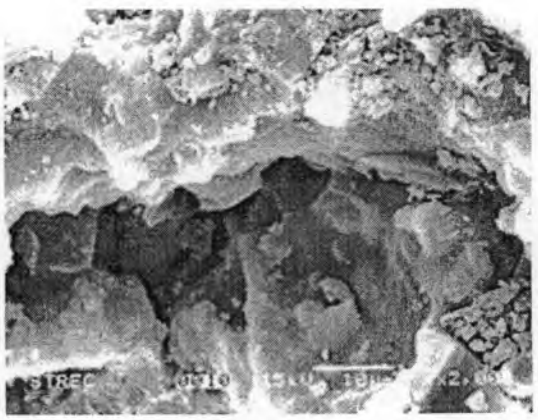

(f)

Figure 4.2 SEM photomicrographs of activated carbon products at various activation temperatures: (a) 350°C (b) 400°C (c) 450°C (d) 500°C (e) 550°C and (f) 600°C

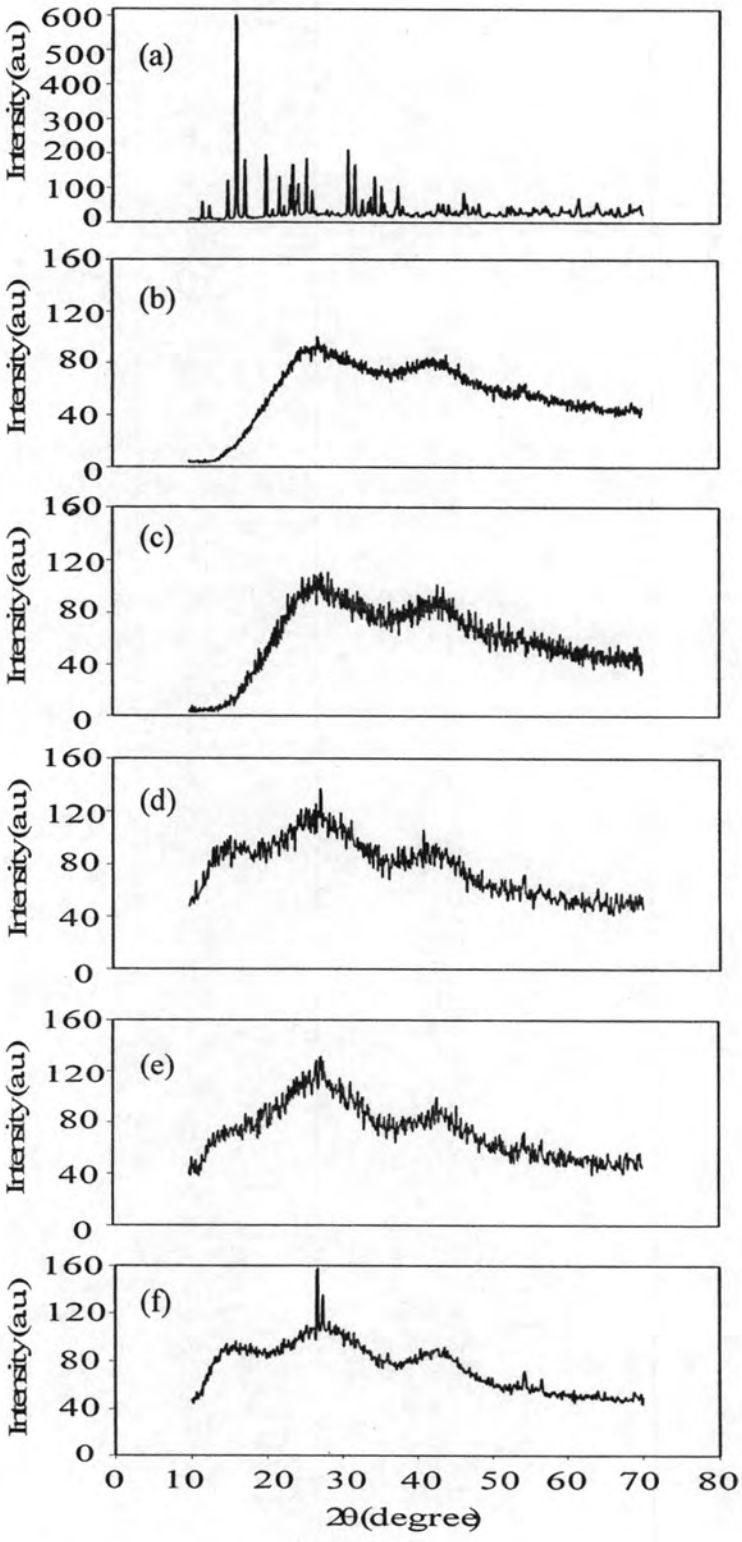

Figure 4.3 XRD patterns of activated carbon products at various activation temperatures: (a) 350°C (b) 400°C (c) 450°C (d) 500°C (e) 550°C and (f) 600°C

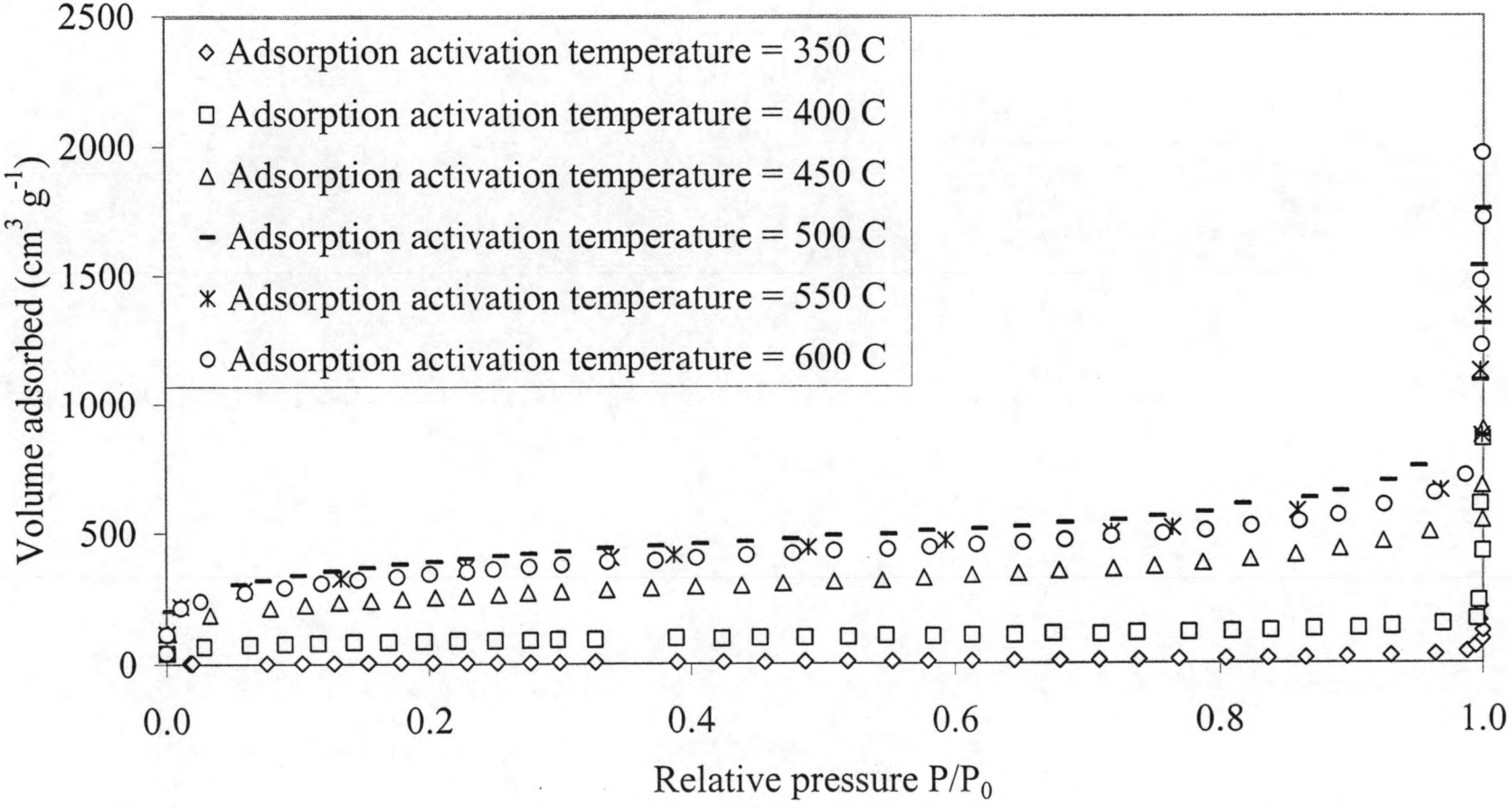

Figure 4.4 Adsorption isotherms of N_2 at -196°C on activated carbon prepared at various activation temperatures

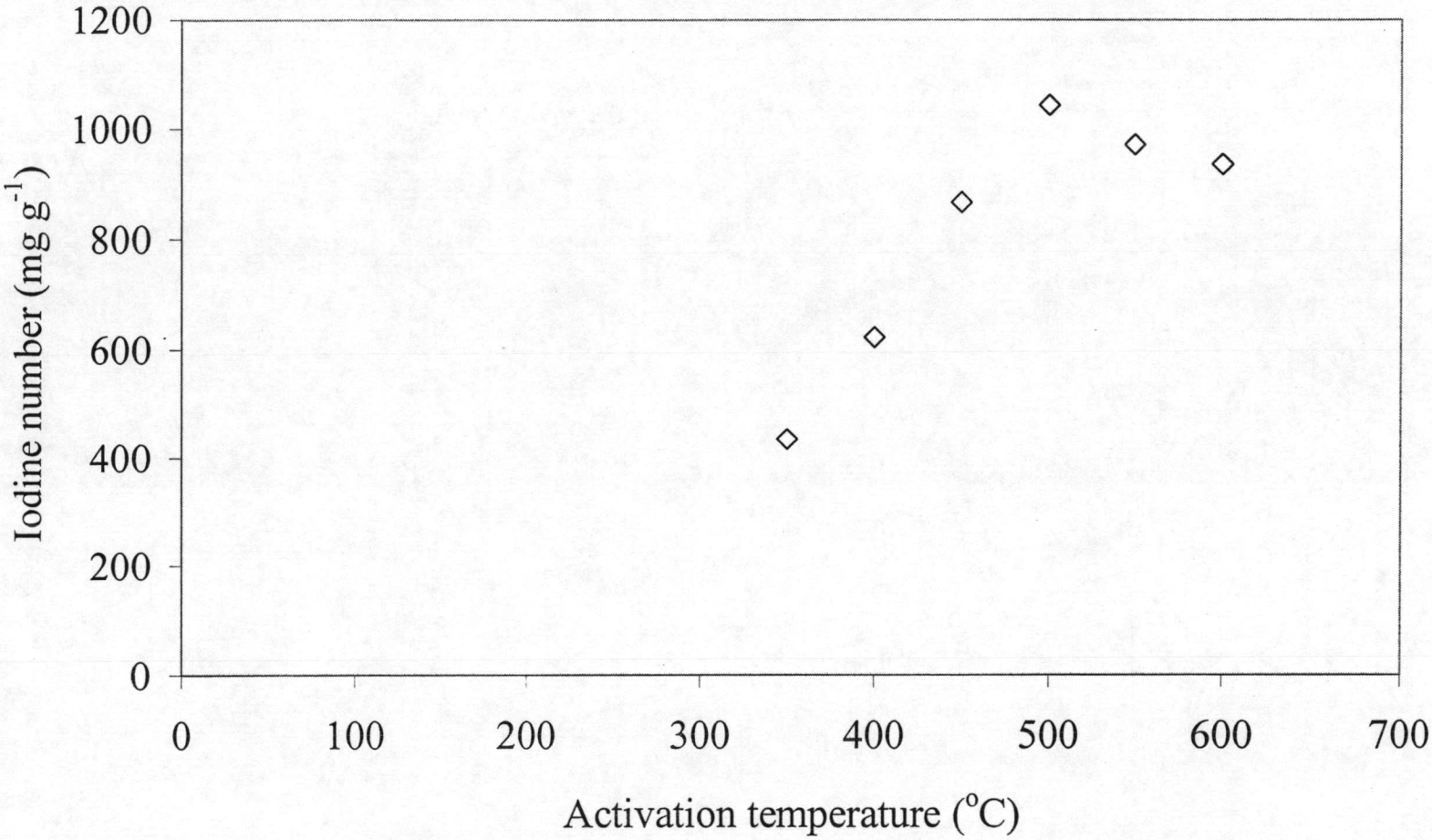

Figure 4.5 Effect of activation temperature on iodine number

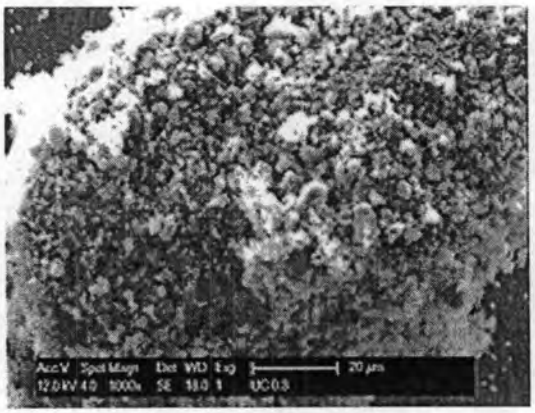

(a)

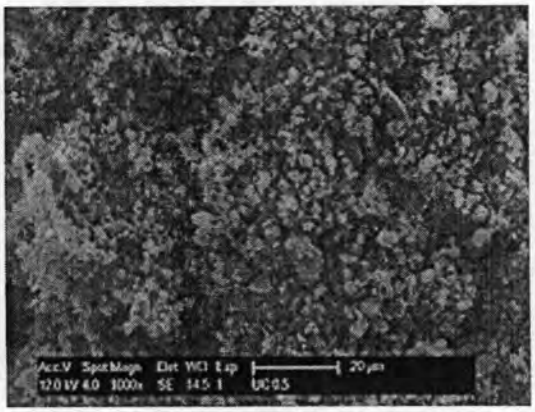

(b)

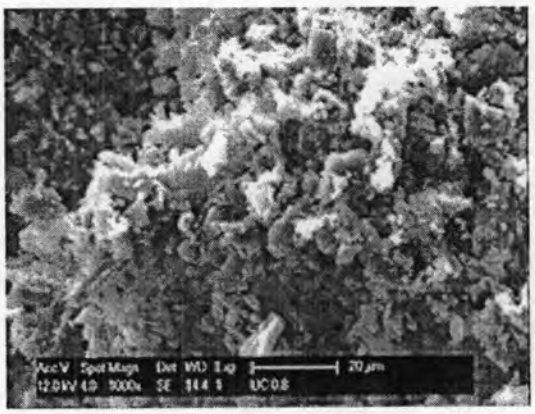

(c)

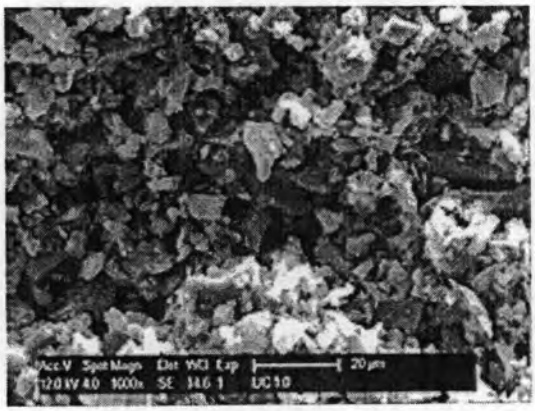

(d)

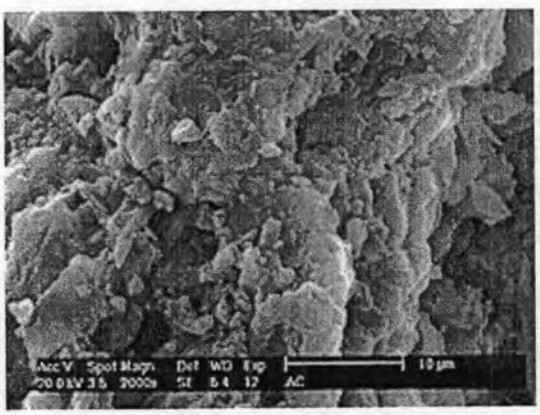

(e)

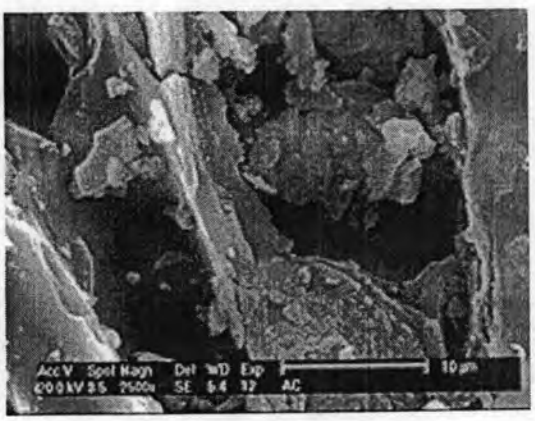

(f)

Figure 4.6 SEM photomicrographs of activated carbon products at impregnation ratios of:

(a) 1:0.3 (b) 1:0.5 (c) 1:0.8 (d) 1:1.0 (e) 1:2.0 and (f) 1:3.0

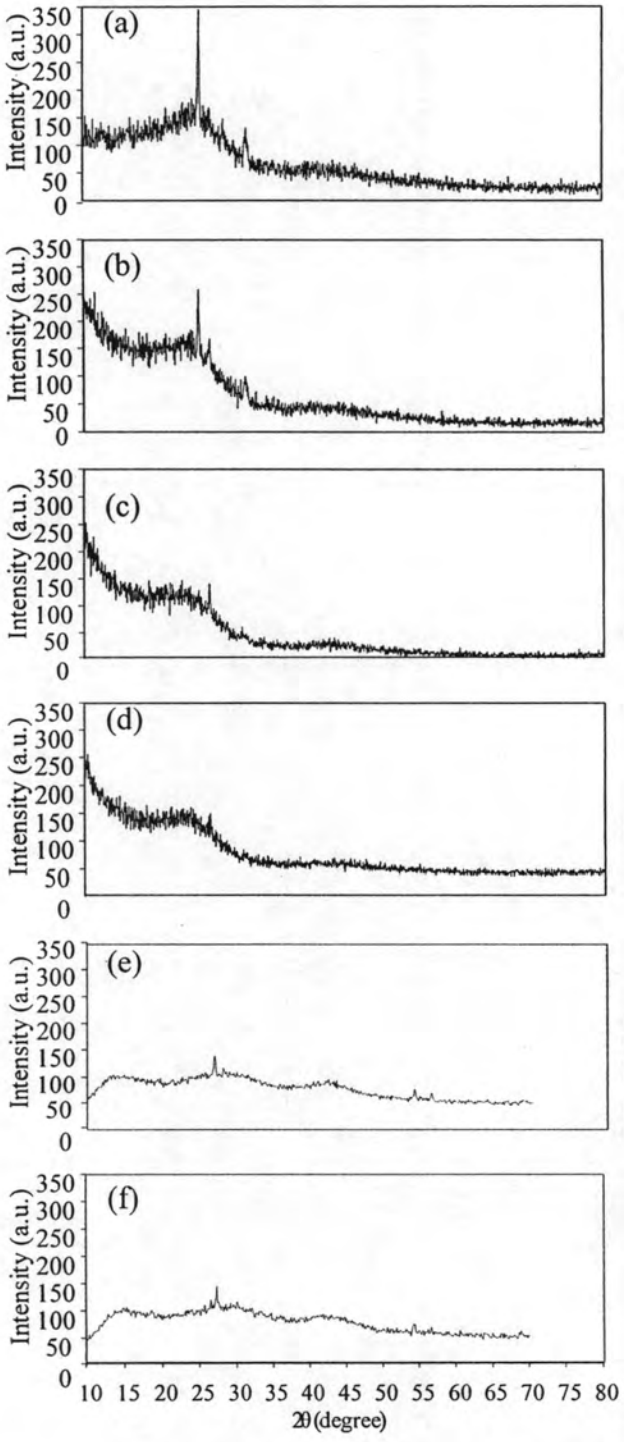

Figure 4.7 XRD patterns of activated carbon products at impregnation ratios of: (a) 1:0.3 (b) 1:0.5 (c) 1:0.8 (d) 1:1.0 (e) 1:2.0 and (f) 1:3.0

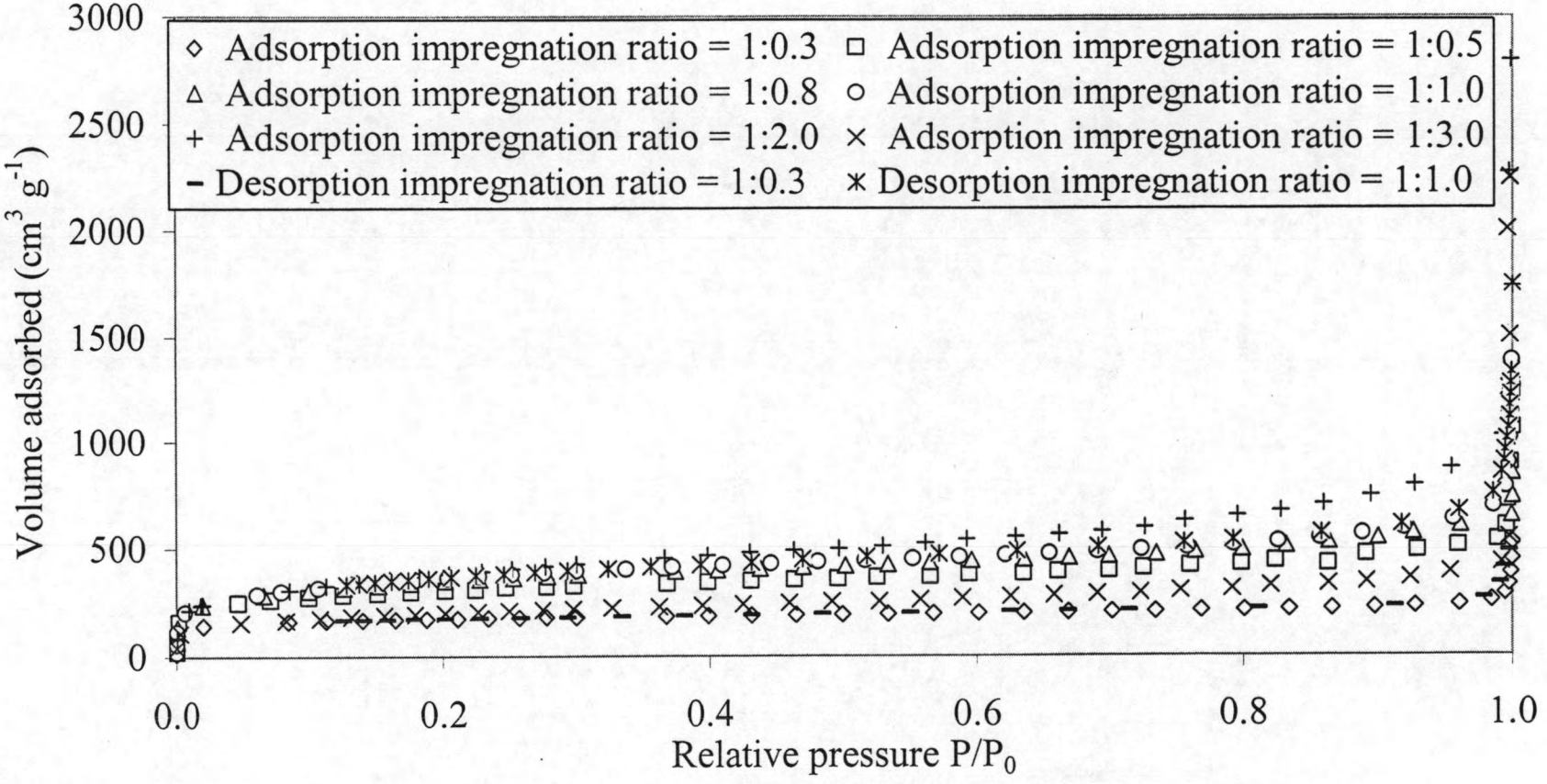

Figure 4.8 Adsorption isotherms of N_2 at -196°C on activated carbon prepared at various impregnation ratios

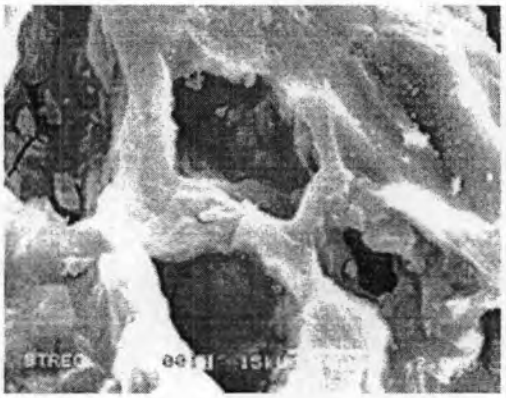

(a)

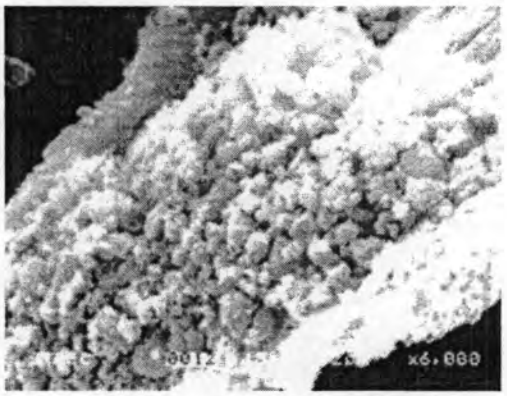

(b)

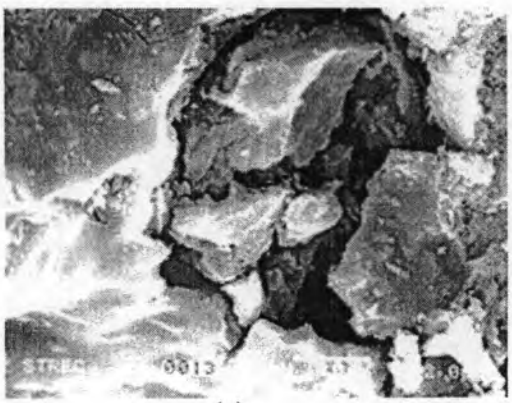

(c)

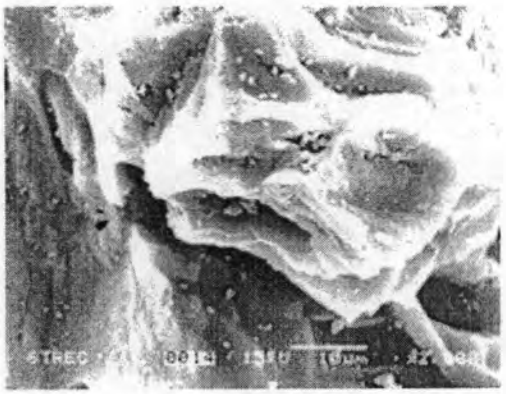

(d)

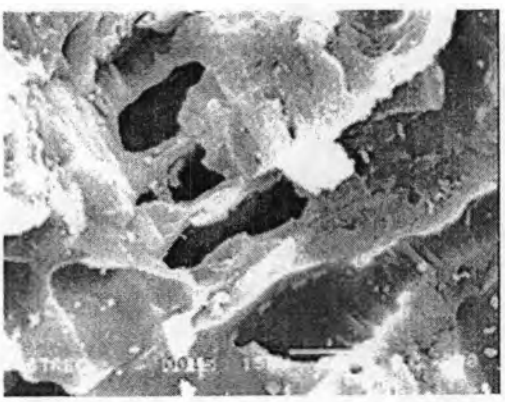

(e)

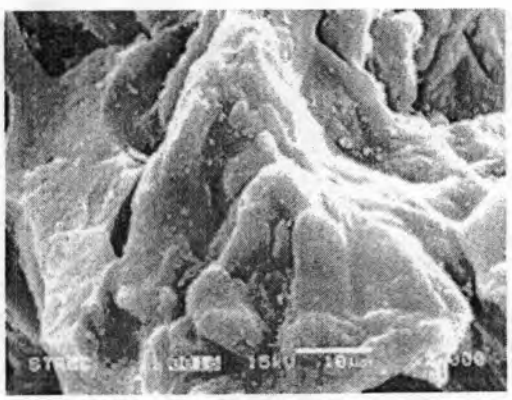

(f)

Figure 4.9 SEM photomicrographs of activated carbon products at various activation times: (a) 0.5 h (b) 1.0 h (c) 1.5 h (d) 2.0 h (c) 2.5 h and (d) 3.0 h

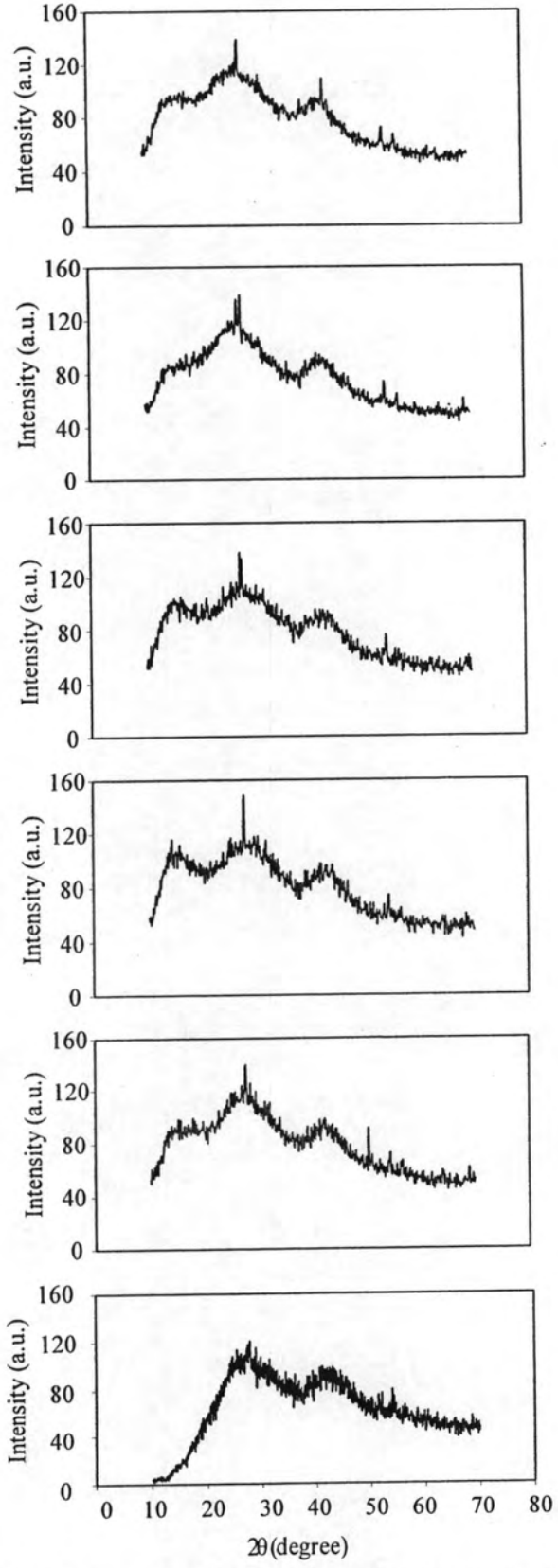

Figure 4.10 XRD patterns of activated carbon products at various activation times: (a) 0.5 h (b) 1.0 h (c) 1.5 h (d) 2.0 h (e) 2.5 h and (f) 3.0 h

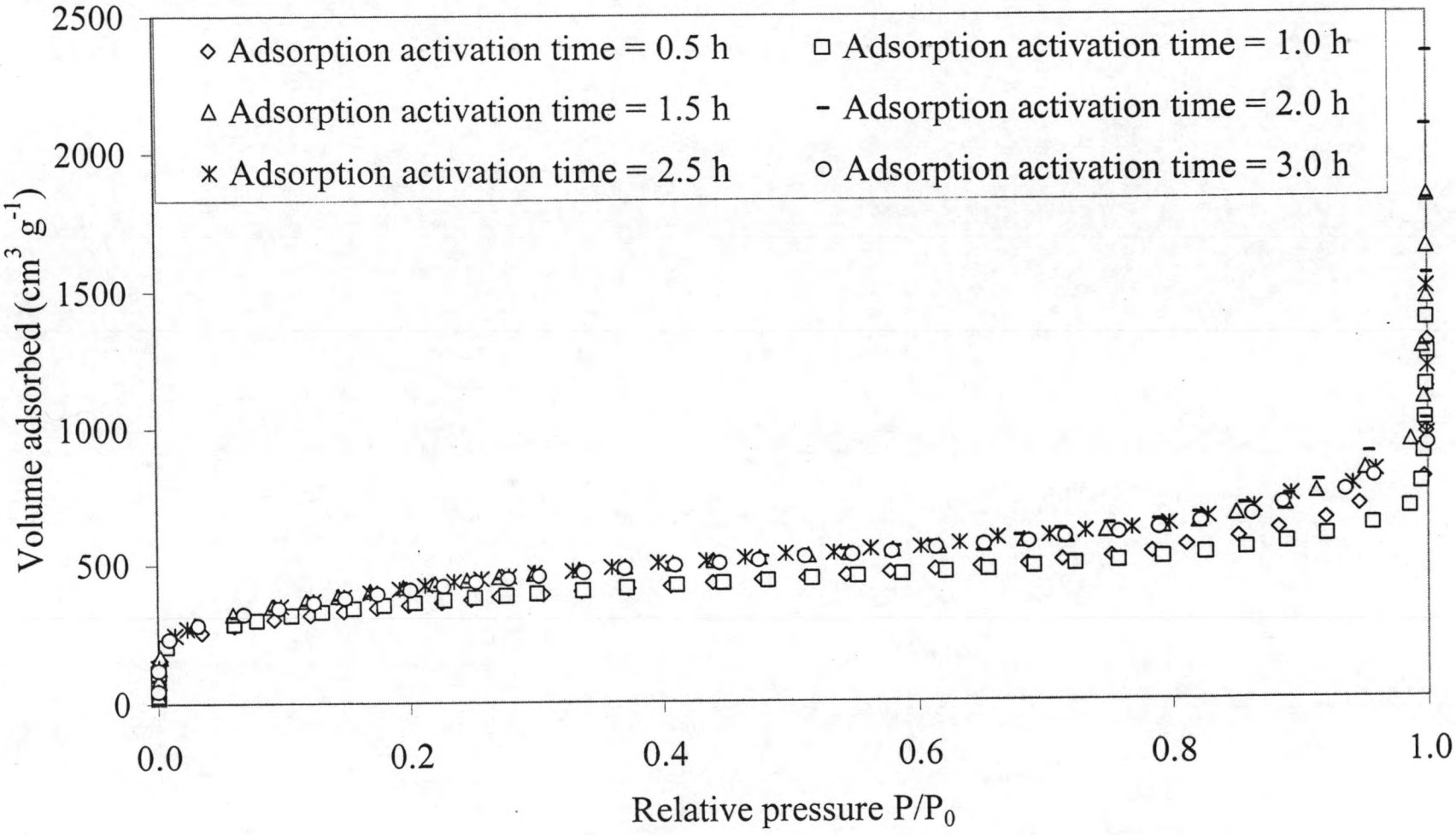

Figure 4.11 Adsorption isotherms of N_2 at -196°C on activated carbon prepared at various activation times